

# Flame speed measurement in H<sub>2</sub>-N<sub>2</sub>O-Ar mixtures

R. Mével<sup>1,2,\*</sup>, F. Lafosse<sup>1</sup>, N. Chaumeix<sup>1</sup>, G. Dupré<sup>1,2</sup> and C.-E. Paillard<sup>1,2</sup>

<sup>1</sup>Institut de Combustion, Aérothermique, Réactivité et Environnement

<sup>2</sup>University of Orléans

## Abstract

Hydrogen-nitrous oxide mixtures are potentially hazardous for nuclear waste storage and semi-conductor manufacturing processes. This system has been studied for decades and numerous fundamental data are available in the litterature. However, flame speed data are quite limited compared to more common mixtures. The purpose of the present study is to obtain additional data on the flame speed of hydrogen-nitrous oxide mixtures and to test the validity of several detailed kinetic schemes. The flame speed of H<sub>2</sub>-N<sub>2</sub>O mixtures 60% Ar diluted has been mesured in a spherical bomb over the equivalence ratio range 0.3-1.8. The initial pressure and temperature are ambiant. It is shown that the flame speed is relatively high with a maximum around 56 cm/s for the stoichiometric mixture. The modeeling results show that the different models tested give a relatively good estimate of the experimental data.

## Introduction

In the nineties, several investigations have shown that nuclear wastes stored at Anford site periodically release a gaseous mixture mainly composed of hydrogen and of nitrous oxide [1–5]. In this frame, many studies have been performed, notably at Caltech [6–11] and at the US Bureau of Mines [12]. The interest on hydrogen-nitrous oxide mixtures would also extend to the semi-conductor industry since their kinetics would play an important role in the oxidation of silane by nitrous oxide, which are widely used in this industry [13].

From Caltech and US Bureau of Mines works, many fundamental parameters, such as flammability limits and detonation cell size, have been derived. However, laminar flame speed data comes from relatively old studies [14–19]. Parker and Wolfhard [14] measured the evolution of the flame speed as a function of pressure in the range 2.4 et 101 kPa. They used the Bunsen burner method and derived the flame surface from the internal luminous cone. Dixon-Lewis et al. [15] studied hydrogen-nitrous oxide-nitrogen mixtures by following magnesium particle trajectories under stroboscopic illumination in a flat flame burner. The temperature is of 291 K and the pressure of 101 kPa. Duval and Van Tiggelen [16] performed an extensive study on the flame speed of H<sub>2</sub>-N<sub>2</sub>O mixtures diluted with various gases (i.e. N<sub>2</sub>, CO, Ar and He). The effects of the initial temperature, of equivalence ratio and of the diluent amount have been investigate at atmospheric pressure. The Bunsen method have been used and

the flame surface is derived from a schlieren visualization. Gray et al. [17, 18] measured the flame speed of non-diluted and NO, N<sub>2</sub> or Ar diluted mixtures as a function of diluent percentage and equivalence ratio. They used a 20 cm long glass cylinder with a inner diameter of 20 cm and a schlieren method. Gray's data have been later corrected by Brown and Smith by applying a numerical procedure described in [19].

From this bibliographic review, it can be concluded that the data on flame speed of hydrogen-nitrous oxide mixtures is quite limited compared to more common mixtures such as hydrogen-air. Moreover, the experimental methods used in the previous studies do not permit to investigate the flame stretch behavior.

## Specific Objectives

The first purpose of this study is to obtain additional data on the flame speed and to derive Markstein lengths, which characterize the flame response to stretch, of hydrogen-nitrous oxide mixtures. Second, this work aims at testing the validity of several detailed kinetic models, the model of Mével et al. [20, 21], the model of Mueller et al. [22] and the model of Konnov [23].

## Materials and Methods

### Materials

Hydrogen-nitrous oxide-argon mixtures were prepared thanks to the partial pressure method from research grade gases supplied by Air Liquide. The equivalence ratio was varied between 0.3 and 1.8. The

---

\*Corresponding author: mevel@cnsr-orleans.fr  
Proceedings of the European Combustion Meeting 2009

Ar dilution was held constant at 60 % for safety purpose. The initial temperature was between 296 and 304 K and the pressure was atmospheric.

Flame speed measurements were performed in a 8-L stainless-steel spherical bomb [24, 25]. The bomb inner diameter is 250 mm. Two quartz optical windows, with a 70 mm diameter and a 40 mm thickness, are mounted opposite to each other and allow the visualisation of the flame. The ignition of the combustible mixtures at the center of the bomb was assured by two electrodes (dia. 2 mm) located along a diameter. The electrodes are linked to a high-voltage source and input power was monitored by measuring the voltage and the current via adapted probes. Prior each experiment, the bomb was pump down to less than 2 Pa. Figure 1 presents the experimental set-up.

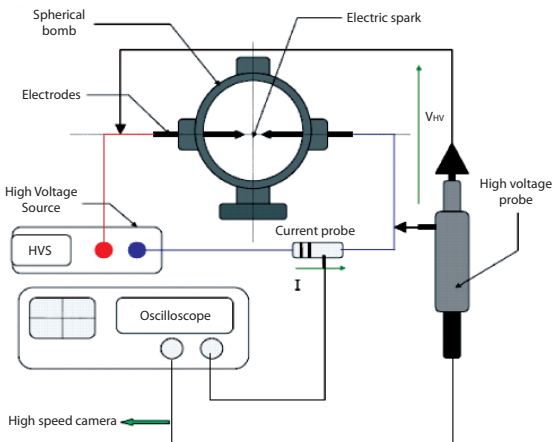


Figure 1: Spherical bomb set-up.

The flame visualisation was achieved via the classical schlieren method. The source light is a 150 W white continuous Xenon lamp from Lot Oriel. The source light is made punctual by passing successively through a plano-convex lens and a bi-convex lens. Diameters and focal lengths of the lenses are ( $f = 250$  mm ; dia = 50 mm) and ( $f = 22$  mm ; dia = 25 mm), respectively. After reflexion on a concave spherical mirror, the light crosses the bomb and is projected on a screen by another concave spherical mirror, after cutting. The mirrors have a diameter of 100 mm and a focal length of 50 cm. The expanding flame propagation is recorded by a Kodak high speed camera with an acquisition frequency of 4500 images/s.

## Methods

The experimentally observed spatial flame velocity corresponds to the stretched one. For a spherical expanding flame, the local stretch effects are due to curvature and strain rate and, as long as the stretch rate is low, the stretched spatial flame veloc-

ity,  $V_S = dR_f/dt$ , is related to the unstretched one as follows :

$$V_S = V_S^0 - L \cdot K \quad (1)$$

In Equation 1,  $L$  is the Markstein length and  $K$  is the stretch rate. For spherical expanding flames,  $K$  is well known and is given by [24, 26] :

$$K = 2 \cdot \frac{V_S}{R_f} \quad (2)$$

By combining Equation 1 and Equation 2, one can obtain, after integration, the unstretched flame spatial velocity as a function of time and of the flame radius :

$$V_S^0 \cdot t = R_f + 2 \cdot L \cdot \ln(R_f) + Cst \quad (3)$$

Knowing the flame radius as a function of time,  $V_S^0$  can be simply derived from an unconstrained least-square regression.

In this study, a home-made Matlab routine has been implemented in order to obtain the flame speed from the schlieren pictures.

## Results and Discussion

### Experimental

Figure 2 presents the evolution of hydrogen-nitrous oxide mixture flame speed as a function equivalence ratio. From this curve it can be noted that the maximum flame speed is achieved for the stoichiometric mixture. It can also be noted that the flame speed decreases more rapidly with equivalence on the lean side than on the rich side. This latter feature is usually observed for flame speed.

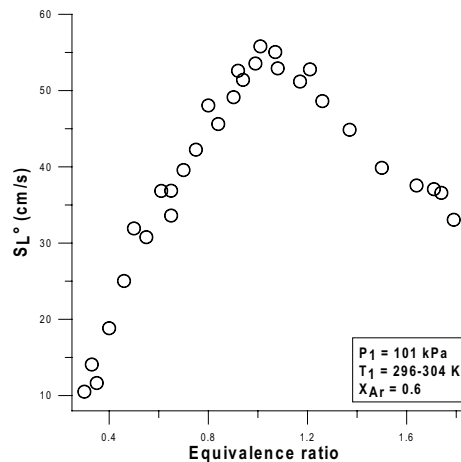


Figure 2: Evolution of hydrogen-nitrous oxide mixtures flame speed as a function of equivalence ratio.

As the equivalence is set-up lower than 0.3, the propagation is not isotrope anymore. This feature

is illustrated on Figure 3. On the frame of the left, it can be seen that the flame propagation is slower on the downward direction. On the frame of the right, the flame can no longer propagate in the downward direction. These observations are indicative of the lean downward flammability limit. For rich mixtures, such a feature has not been observed and the ignition is not possible for mixtures with equivalence ratio higher than 1.8.

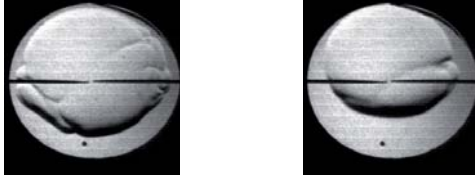


Figure 3: Evidence of the lean downward flammability limit.  $P_{ini} = 101 \text{ kPa}$ ;  $T_{ini} = \text{ambient}$ . Frame on the left:  $\Phi = 0.25$ ; Frame on the right:  $\Phi = 0.2$

Figure 4 shows the evolution of the Markstein lengths as a function of equivalence ratio.

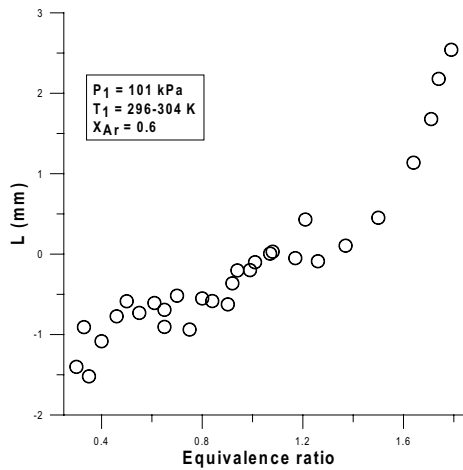


Figure 4: Evolution of hydrogen-nitrous oxide mixtures Markstein lengths as a function of equivalence ratio.

It can be seen that the values of Markstein lengths extend over a wide domain (-1.5 to 2.5) corresponding to a variety of flame as seen on Figure 5. For lean mixtures, frames of the left, Markstein lengths are negative and thus flames are unstable with respect to thermo-diffusive instabilities. Lean flames appear as cracked surfaces with cell development. As the flame is stoichiometric, Markstein lengths tend to zero and the flame front appears as a smooth continuous surface (frames of the center). For rich mixtures, the Markstein lengths are highly positive and flames are stabilised (frames of the right).

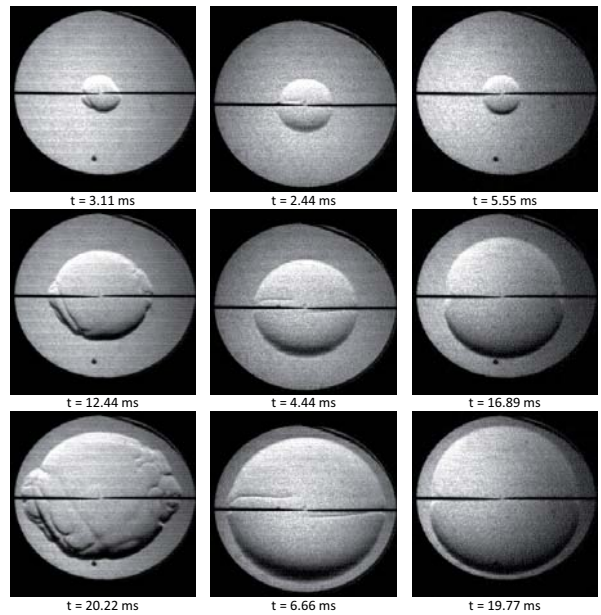


Figure 5: Schlieren photographs of hydrogen-nitrous oxide flames of different equivalence ratios.  $P_{ini} = 101 \text{ kPa}$ ;  $T_{ini} = \text{ambient}$ . Frames on the left:  $\Phi = 0.33$ ; Frames on the center:  $\Phi = 1.01$ ; Frames on the right:  $\Phi = 1.74$

### Modelling

The modelling of the present experimental results has been performed by using the Cantera software [27]. The kinetic schemes used were the models of Mével et al. [20, 21], the model of Mueller et al. [22] and the model of Konnov [23].

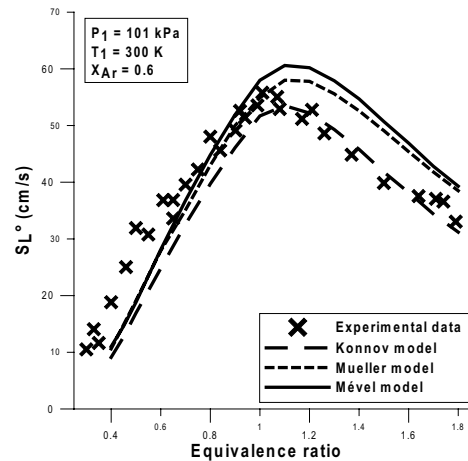


Figure 6: Modelling of the flame speed in hydrogen-nitrous oxide-argon mixtures.  $P_{ini} = 101 \text{ kPa}$ ;  $T_{ini} = 300 \text{ K}$ ;  $X_{Ar} = 0.6 \text{ K}$ .

Figure 6 shows the results of this modelling. It can be seen that the three models give a relatively good estimate of the flame speed. The model of Mével is the fastest one. It overestimates the flame speed for rich mixtures but gives better results for the lean

mixtures. The results obtained with the model of Mueller are quite similar that those of the model of Mével but the results are slightly better are the rich mixtures. Finally, it can be seen that the prediction of the model of Konnov are excellent for rich mixtures but are not that good in the lean side. In order to extend the comparison between the three models, the experimental results of Gray et al. [18] and those corrected by Brown and Smith [19] have been also modelled. Figure 7 presents the results of this modelling. For this set of experimental data, the prediction given by the different models are quite similar. The models of Mueller and of Konnov predict the same flame speed within a few cm/s all over the composition conditions examined. The results of the model of Mével are somehow faster for mixtures with equivalence ratio higher than 0.6 but remain consistent with the experimental data.

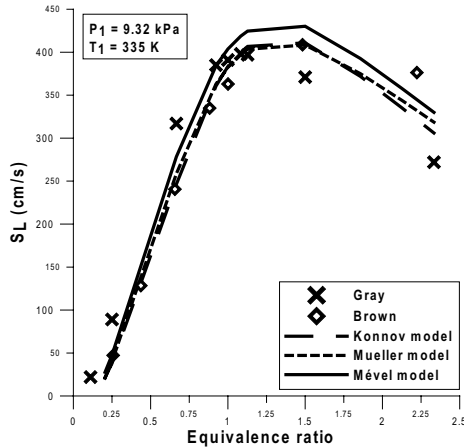


Figure 7: Modelling of the flame speed in hydrogen-nitrous oxide mixtures.  $P_{ini} = 9.33$  kPa ;  $T_{ini} = 335$  K.

In order to investigate the kinetics of the system, sensitivity and reaction pathway analysis have been carried out using the Cosilab software [28].

The sensitivity analysis has been performed with respect to the flame speed and to the temperature. Figure 8 shows an example of the results obtained for a stoichiometric flame. It can be seen that the most important reaction for the flame speed and the temperature is  $N_2O+H=N_2+OH$ . The reaction  $N_2O+H=NH+NO$ , which competes for H consumption with the reaction  $N_2O+H=N_2+OH$ , possesses a high negative coefficient. The reaction  $H_2+OH=H_2O+H$ , which regenerate H atoms, enhances the flame speed and the temperature increase. The two reactions  $NH+OH=HNO+H$  and  $NH+NO=N_2+OH$ , which compete for radicals consumption, are also important reactions.

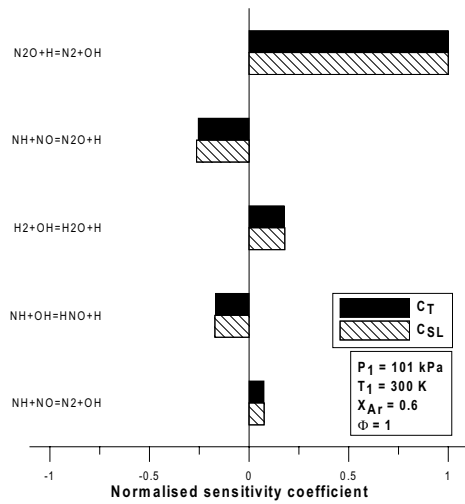


Figure 8: Normalised sensitivity coefficient with respect to the flame speed and to the temperature.  $\Phi = 1$  ;  $P_{ini} = 101$  kPa ;  $T_{ini} = 300$  K ;  $X_{Ar} = 0.6$  K.  $C_T$  : Sensitivity coefficient on the temperature ;  $C_{SL}$  : Sensitivity coefficient on the flame speed.

The reaction pathway analysis have been performed for H, O and N elements. Figure 9 and Figure 10 shows the results obtained for H and O containing species in the case of a stoichiometric flame. Note that these two graphs have been obtained by integrating the element fluxes along the flame thickness.

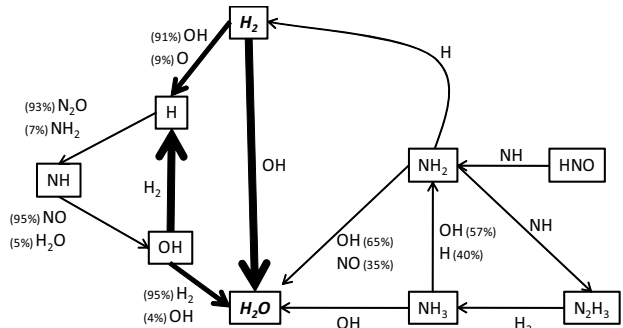


Figure 9: Reaction pathway analysis with respect to H element.  $\Phi = 1$  ;  $P_{ini} = 101$  kPa ;  $T_{ini} = 300$  K ;  $X_{Ar} = 0.6$  K.

For the stoichiometric mixture, the quasi-totality of the N element is converted from  $N_2O$  into  $N_2$ . The reaction responsible for this conversion is  $N_2O+H=N_2+OH$ . It can also be noted that a little amount of  $N_2O$  is converted into  $NO$  and  $NH$  through the reaction  $N_2O+H=NO+NH$ . The O element are converted from  $N_2O$  into  $H_2O$  through the sequence:  $N_2O+H=N_2+OH$ ,  $OH+H_2=H_2O+H$ . Little amounts of O atoms are converted from  $N_2O$  into  $NO$  by the reaction  $N_2O+H=NO+NH$ . The decomposition of nitrous oxide has only a small participation in the conversion of the O element from  $N_2O$  into

$H_2O$  through the sequence:  $N_2O(+M)=N_2+O(+M)$ ,  $O+H_2=OH+H$ ,  $OH+H_2=H_2O+H$ . For the H element, it can be noted that a large proportion of the initial hydrogen molecules react with OH radicals to form  $H_2O$ .

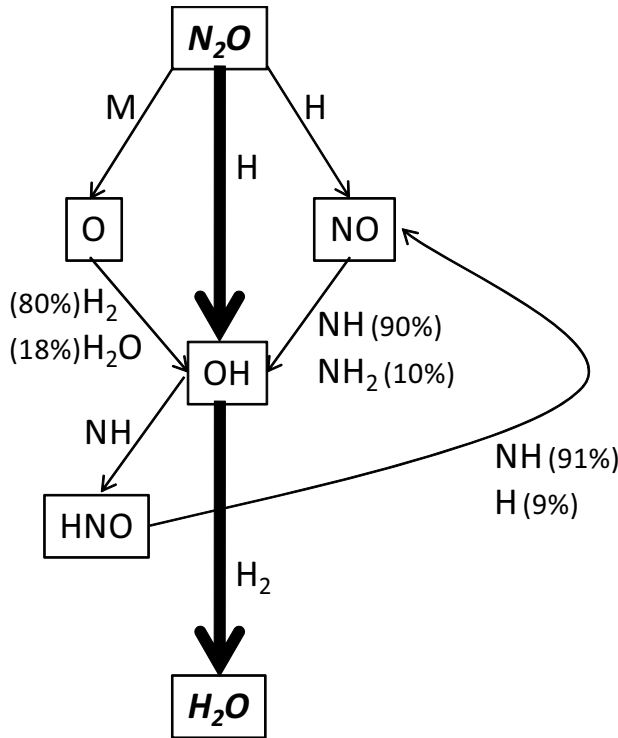


Figure 10: Reaction pathway analysis with respect to O element.  $\Phi = 1$ ;  $P_{ini} = 101$  kPa;  $T_{ini} = 300$  K;  $X_{Ar} = 0.6$  K.

From the sensitivity and the reaction pathway analysis it can be noted that the reaction  $N_2O+H=N_2+OH$  dominates the chemistry of  $H_2-N_2O$  mixtures. In order to illustrate this feature, the flame speed has been calculated with the Mueller model in which the rate constant of the reaction  $N_2O+H=N_2+OH$  has been multiply and divided by two. The results obtained are shown in Figure 11. The reaction  $N_2O+H=N_2+OH$  is the most important for the temperature increase since it is highly exothermic and that it forms OH radicals which further react with  $H_2$  to produce  $H_2O$  and involve an additional heat release. Such a feature has been also observed for auto-ignition of  $H_2-N_2O$  mixtures [20]. On the contrary to auto-ignition processes, the thermal decomposition of nitrous oxide has a very small importance for flame propagation. This can be explained by the diffusion of H atoms ahead of the flame front. Indeed, for auto-ignition to occur, it is necessary that the reactants first break. Since the H-H bond is very strong,  $N_2O$  decomposes before  $H_2$  and release O atoms which react with

hydrogen molecule to release H atoms. These atoms then react with nitrous oxide through the reaction  $N_2O+H=N_2+OH$  and are regenerated by reacting with hydrogen molecule leading to a fast energy release through a linear chain. In propagating flames, H atoms diffuse ahead of the flame front and react with nitrous oxide mainly through the reaction  $N_2O+H=N_2+OH$  allowing the energy to be released. Thus the pathway  $N_2O(+M)=N_2+O(+M)$ ,  $O+H_2=OH+H$  is almost suppressed because of the H atoms diffusion.

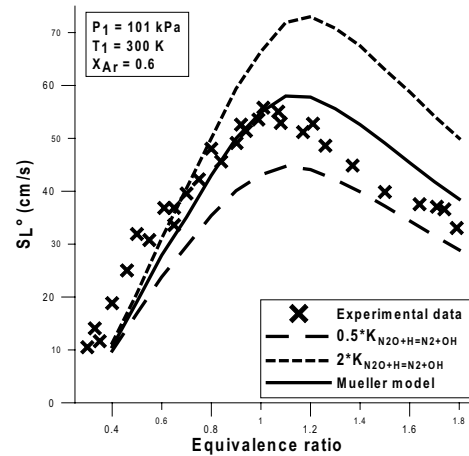


Figure 11: Effect of the value of the rate constant of  $N_2O+H=N_2+OH$  on the modelling of the flame speed in hydrogen-nitrous oxide-argon mixtures.  $P_{ini} = 101$  kPa;  $T_{ini} = 300$  K;  $X_{Ar} = 0.6$  K.

## Conclusions

In the present study, the flame speed of hydrogen-nitrous oxide 60% Ar diluted has been measured at ambient temperature and pressure conditions over the equivalence ratio 0.3-1.8. It is shown that these flames are relatively fast with a maximum around 56 cm/s for the stoichiometric mixture. The modelling of these experimental data has been performed with three recently developed models. All the kinetic schemes gives satisfactory predictions of the experimentally observed data. Sensitivity and reaction pathway analysis have demonstrate that the dynamic of the system is dominated by the reaction  $N_2O+H=N_2+OH$  which governs the energy release rate.

## Acknowledgements

This work was partly supported by the French " Ministère de l'Éducation Nationale, de l'Enseignement Supérieur et de la Recherche ". The authors wish to acknowledge Ludovic Landry (from LME-Polytech Orléans) and Kirsten Leistner (from University of Benevento) for usefull cooperation in the Matlab flame speed routine implementation.

## References

- [1] MacFarlane D., Bott T., Brown L., Stack D., Kindinger J., Deremer R., Medhekar S. and Miskschl T., in Proceeding of the PSAM-II Conference, 101 Risk Assessment of Nuclear Waste Storage and Processing, pp. 1–6.
- [2] Roblyer S., Finfrock S. and Powell W., in Proceedings of the International Conference: Mathematics and Computations, Reactor Physics, and Environmental Analyses, pp. 225–234.
- [3] Titzler P., Legare D. and Barrus H., Trans. Am. Nucl. Soc., 69 (1993) 484.
- [4] Fox G. and Stepnewski D., Trans. Am. Nucl. Soc., 70 (1994) 85–86.
- [5] Bryan S., King C. and Pederson L., Trans. Am. Nucl. Soc., 81 (1999) 97–99.
- [6] Akbar R., Kaneshige M., Schultz E. and Shepherd J., Tech. Rep. FM-97-3, Explosion Dynamics Laboratory, California Institute of Technology (1997).
- [7] Kaneshige M., Schultz E., Pfahl U., Shepherd J. and Akbar R., in Proceedings of the 22<sup>nd</sup> International Symposium on Shock Waves, vol. 1, pp. 251–256.
- [8] Liang Z., Karnesky J. and Shepherd J., Tech. Rep. FM-2006-003, Graduate Aeronautical Laboratories, California Institute of Technology (2006).
- [9] Pfahl U., Ross M. and Shepherd J., Combust. Flame, 123 (2000) 140–158.
- [10] Pfahl U., Schultz E. and Shepherd J., Tech. Rep. FM-98-5, Graduate Aeronautical Laboratories, California Institute of Technology (1998).
- [11] Ross M. and Shepherd J., Tech. Rep. FM96-4, Graduate Aeronautical Laboratories, California Institute of Technology (1996).
- [12] Cashdollar K., Hertzberg M., Zlochower I., Lucci C., Grenn G. and Thomas R., Tech. Rep. WHC-SD-WM-ES-219, Pittsburgh Research Center (1992).
- [13] Mick H. and Roth P., J. phys. chem., 98 (1994) 5310–5313.
- [14] Parker W. and Wolfhard H., Proc. Combust. Inst., 4 (1953) 420–428.
- [15] Dixon-Lewis G., Sutton M. and Williams A., Combust. Flame, 8 (1964) 85–87.
- [16] Duval A. and Van Tiggelen P., Bul. Aca. R. Belges, 53 (1967) 366–402.
- [17] Gray P., Mackinven R. and Smith D., Combust. Flame, 11 (1967) 217–226.
- [18] Gray P., Holland S. and Smith D., Combust. Flame, 14 (1970) 361–374.
- [19] Brown M. and Smith D., Proc. Combust. Inst., 25 (1994) 1011–1018.
- [20] Mével R., Javoy S., Lafosse F., Chaumeix N., Dupré G. and Paillard C.E., Proc. Combust. Inst., 32 (2009).
- [21] Javoy S., Mével R. and Paillard C.E., Int. j. chem. kinet., (In press).
- [22] Mueller M., Yetter R. and Dryer F., Int. j. chem. kinet., 31 (1999) 704724.
- [23] Konnov A., Detailed reaction mechanism for small hydrocarbons combustion. release 0.5. (2000).
- [24] Lamoureux N., Djebaïli-Chaumeix N. and Paillard C., Exp. therm. fluid sci., 27 (2003) 385–393.
- [25] Halter F., Chauveau C., Djebaïli-Chaumeix N. and Gökalp I., Proc. Combust. Inst., 30 (2005) 201–208.
- [26] Aung K., Hassan M. and Faeth G., Combust. Flame, 109 (1997) 1–24.
- [27] Goodwin D., Tech. rep., California Institute of Technology (2005).
- [28] COSILAB, Tech. rep., SoftPredict, Roxeto GmbH & Co (2007).